EXPERIMETNAL STUDY ON BURNING BEHAVIORS OF LIQUID FUELS WITH DIFFERENT SOOTING LEVELS AT HIGH ALTITUDE

Jiahao LIU[1,2], Pan LI[1], Mingyi CHEN[1], Xiao CHEN[1], Richard YUEN[2], Jian WANG[1,*]

[1]State Key Laboratory of Fire Science, University of Science and Technology of China, Hefei, China;
[2]Department of Architectural and Civil Engineering, City University of Hong Kong, Hong Kong, China.

[*]Author for correspondence: wangj@ustc.edu.cn, Tel: 86 551 63606463

Abstract

To validate the feasibility of classical fire scaling laws under low pressure, three typical liquid fuels with different sooting levels, i.e. ethanol, n-heptane and jet-A, were employed in this paper to perform a sequence of pool fires in a high-altitude city, Lhasa (3650 m, 64.3 kPa). Mass loss, axial temperature profile and radiative heat flux were recorded in each test. From the assessment of experimental data, it can be concluded that the dimensionless burning intensity $\dot{m}''\mu/D$ can be correlated against the Grashof number to different powers for all the three fuels, and the exponent increases with the sooting level of fuels. A correlated relationship expressed as $\Delta T \sim [z(P/Q)^{2/5}]^{\eta}$ can be applied to analyze the axial temperature rises, partitioning flame region, intermittent region and plume region with the modified demarcations, i.e. 0.42 and 1.06. In addition, the averaged flame temperature grows higher with declining sooting level of fuels, while the radiative heat fluxes exhibit the opposite results. Moreover, the measured radiative heat fluxes for different fuels are proportional to $L_m T_f^5$, and the soot volume fraction apparently increases with the sooting level of the fuels under low pressure condition.

Key words: *burning intensity; high altitude; pool fire; sooting level*

1. Introduction

Numerous experiments, including field and chamber tests, have demonstrated that the ambient pressure significantly affects the burning process [1-8]. Most of the bench-scale experiments examining the pressure effect on fire behaviors tend to be achieved by the man-made pressure chambers, which are usually constrained by the unstable inner environment, especially for relatively large-scale fires. Another available method to create low-pressure condition is to perform experiments at high altitude [1-7] or by utilizing a helicopter [8]. Compared with chamber test, the field test provides a more steady low pressure environment and more reliable conclusions. With the completion of fire laboratory in Lhasa (altitude 3650 m, ambient pressure 64.3 kPa), a series of experiments were conducted to investigate the fire behaviors under lower pressure. The fuels employed are mainly

typical combustible liquids (ethanol [4,5], n-heptane [1-5]) and solids (wood crib [2], cardboard box [6,7]). Testified by the abundant experiments, there is a consensus that the burning intensity, thermal radiation and soot formation decrease whereas the maximum flame temperature at a fixed burning rate increases under low pressure.

To develop the scaling model under different pressures, pressure modeling and radiation modeling were proposed by De Ris et al. [9,10] and has been validated by the experimental data obtained under elevated pressures. Pressure modeling, by preserving the *Gr* and *Fr*, has been applied to convection-dominated fires [11,12] and generalized to experimental results under low pressure by previous researchers [7,13]. Radiation modeling [10], based on the assumptions that soot radiation is dominant and a second-order pressure dependence of soot formation rate, indicates that the burning intensity remains constant if holding the product of pressure-squared times characteristic length P^2D invariant. Zhou et al. [13] employed the two scaling models above to analyze the experimental results at high altitude, and summarized that the pressure modeling is more applicable for moderate pool fires and the burning intensity can be correlated as $\dot{m}''D \sim (P^2D^3)^n$, where n = 0.45 for the examined ethanol and n-heptane fires. However, Yao et al. [7] conducted cardboard box fires at high altitude and gained an exponent n = 0.31 which approximated to the theoretical value 1/3.

The diversified exponential factors may be associated to the different sooting-level fuels, which may yield different amount of soot for a given ambient pressure. To confirm the inference, three typical liquid fuels, i.e. ethanol, n-heptane, jet-A, corresponding to weakly-sooting, moderately-sooting and heavily-sooting fuels, respectively, were employed to test pool fire behaviors in Lhasa. The burning intensity for different pool dimensions is correlated with pressure modeling and radiation modeling, and further discussed contrastively. In addition, temperature profile and radiative heat flux are analyzed to improve the understanding of fire behaviors under lower pressure. The knowledge is critical for fire safety engineering design in high-altitude environments and also offers effective guidance to develop fire suppression techniques for different sooting-level fuels at high altitude.

2. Experimental setup

All the experiments were conducted in an EN54 standard combustion room built in Lhasa, the size of which is 10 m long, 7 m wide and 4 m high and can be considered as open space compared with the tested pool dimensions (i.e. circular pans with diameters of 10 cm, 14 cm, 20 cm, 30 cm) in current study. These stainless steel pans are 2 cm in depth and 0.32 cm ± 0.01 cm in thickness. For each test, the liquid fuels were filled to a fuel thickness of 1.5 cm, so the weight of fuel for different pool dimensions could be estimated by the utilization of the density of the fuels. The specific property parameters of the three fuels and experimental configurations are listed in Table 1.

Table 1. Summary of experimental configurations

Fuel	Density (kg/m^3)	Pool sizes (cm)	Ambient conditions		Measurements
Ethanol	789	10, 14, 20, 30	Pressure (kPa)	64.3	➢ Mass loss
N-heptane	679		Temperature (^oC)	10 ± 3	➢ Temperature
Jet-A	792		Relative humidity	15%	➢ Radiation

The experimental setup in current study is illustrated in Fig. 1. The mass loss of the fuel was

measured by an electronic scale with a readability of 0.01 g. A 0.5×0.5 m insulation board was placed between scale and fuel pan to shield the high temperature. A rack of fourteen armored K-type thermocouples with diameter of 0.5 mm were mounted vertically along the axis of the pan. The intervals of the lower eight thermocouples and upper six ones were 5 cm and 10 cm, respectively. To eliminate the radiation effect upon the thermocouples, Luo's method [14] was used to correct the error of the measured temperature and the uncertainty could be less than 10%. Besides, a radiometer flush with the top of the pan was positioned at a distance of 0.3 m away from the pan axis to record the flame radiation. The radiometer manufactured by Medtherm Corporation (USA) is a type of Gardon gauge, which is primarily intended for the measurement of radiation flux density from a field of view of 180 degrees. The responsivity of the sensor is 0.1662 mV per kW m^{-2} with the expanded uncertainty of ± 3%. The sampling rate of all devices was 1 Hz. Each test was repeated at least three times to guarantee the repeatability.

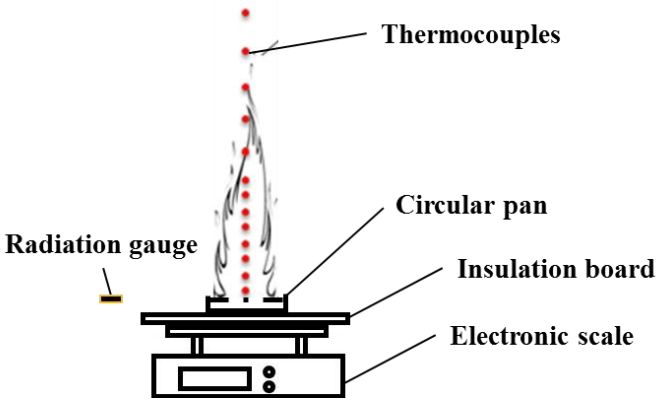

Fig. 1. Experimental setup for pool fire study

3. Results and discussion

According to previous study [1,15,16], the pool fires in current study are assigned to be thin-layer fuel burning process, which can be divided into four typical stages: Ⅰ) pre-steady stage; Ⅱ) quasi-steady stage; Ⅲ) boiling stage; Ⅳ) decay stage. The pre-steady stage refers to the short transition from ignition to quasi-steady stage. In the quasi-steady stage, the heat feedback from the flame reaches a quasi-equilibrium state with the heat for fuel vaporizing and warming up, exhibiting a relatively stable burning rate and flame envelop. With the consumption of the fuel, the combined effects of flame and hot steel container preheat all the residue fuel to the boiling temperature, leading to the violent burning stage, i.e. the boiling stage, where the bubbles are continuously formed on the solid-liquid surface at the bottom of the pan [1,16]. Under such circumstance, the heat exchange will be promoted markedly, leading to a rapidly increased burning rate. When the burning rate reaches to peak, the consumption of the residual fuel together with the reduction of effective fuel surface results in the commencing of the decay stage. Moreover, it is worthwhile to note that the boiling points of liquid fuels tend to decrease with the decreasing ambient pressure. For example, the boiling point of n-heptane fuel at Lhasa is 89 ^{o}C, while that at atmospheric pressure is 98.5 ^{o}C [4]. Thus, the thin-layer pool fires at high altitude are more prone to boil in the combustion process.

In current study, only the quasi-steady stage with stable burning rate and flame envelop was analyzed due to its balanced heat feedback to the fuel surface. Fig. 2 shows the experimental result of 14 cm n-heptane pool fire, where the quasi-steady stage can be identified as the smooth period of the

derivative of mass loss. The criterion of $\left|d\dot{m}''/t\right| \le 0.01\,\mathrm{g\,s^{-2}\,m^{-2}}$ is adopted to identify the range of the quasi-steady burning stage and the occurrence of the boiling stage. All the experimental data are processed in the similar method to acquire the mass loss of different fuels, then the repeated experimental configurations will be averaged to give the ultimate data. Correspondingly, the data of axis temperature profile and flame radiation in the duration of quasi-steady stages can be obtained and assessed.

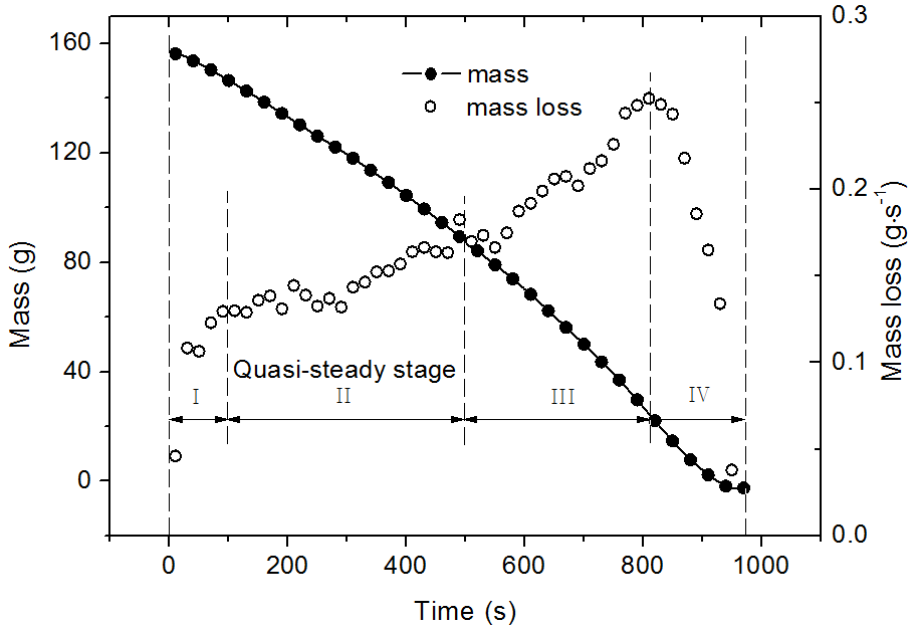

Fig. 2. History of mass loss of 14 cm n-heptane pool fire

3.1 Scaling law of burning intensity

Due to the difficulty of performing large scale fires, researchers tend to conduct down-scaled experiment and further analogize to the expected one via the proper scaling law [17,18]. Mass loss ($\dot{m}$), or burning intensity ($\dot{m}''$) which is defined as the mass loss per unit burning surface area, serves as a key parameter in determining fire hazard for fire safety engineering design, has been widely studied in the fire science. By preserving the dimensionless parameter Grashof number, De Ris et al. [9] proposed the pressure modeling which primarily addressed the scaling law of convection-dominated fires. The expression for pressure modeling can be written as

$$\dot{m}''D/\mu \sim Gr^{\alpha} \tag{1}$$

where μ is viscosity, in $\mathrm{g\,s^{-1}\,m^{-1}}$, α is exponent factor. The radiation modeling [10] is established upon the hypothesis that soot radiation is dominant in heat feedback and acts as a second-order pressure dependence of soot formation. Accordingly, the burning intensity can be correlated with the product of P^2D as

$$\dot{m}'' \sim (P^2D)^{\beta} \tag{2}$$

Through the assessment of the two models above, Zhou et al. [13] indicated that the pressure modeling is more suitable in evaluating the burning intensity of moderate pool fires under low

pressure, and α values for ethanol and n-heptane pool fires appear to be identical, i.e. α =0.45. The pool fires in current study also belong to the moderate ones and can be analyzed by using the pressure modeling. The correlated results for the three fuels are plotted in Fig. 3. It clearly shows that the dimensionless burning intensity can be correlated against the Grashof number with different powers, i.e. 0.35, 0.37, 0.41 for ethanol, n-heptane and jet-A, respectively. Kanury et al. [19] tested eight different polymeric solids in the geometry of horizontal circular pools to deal with steady turbulent free convective diffusional burning under elevated pressures, and concluded that α =1/3 for convection-dominated fires. Based on that, the Eq. (1) can be scaled as follow,

$$\dot{m}''D/\mu \sim Gr^{1/3} \sim (\rho^2 D^3)^{1/3} \sim P^{2/3}D \tag{3}$$

Therefore, the burning intensity is independent of pool dimension under this circumstance. Lockwood and Corlett [20] measured both the convective and the radiative feedback heat flux in small methanol and kerosene fires of 30 cm diameter. An exponent slightly larger than 2/3 was reported for the convective portion at lower pressures, which is also consistent with the acquired α values.

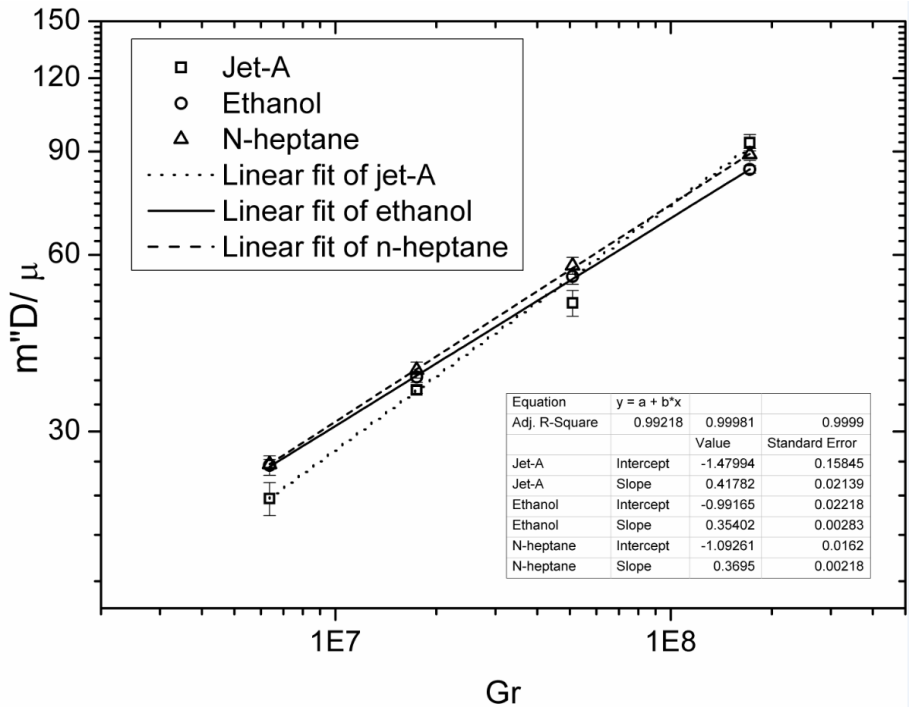

Fig. 3. Burning intensity correlated with pressure modeling

With respect to the radiation modeling which emphasizes the role of soot formation, the current experimental data together with that obtained by De Ris et al. [10] to validate the radiation modeling are plotted in Fig. 4 using the Eq. (2). It shows that the β value for ethanol fires approximates to zero, which reflects an invariant burning intensity for ethanol pool fires. Then, with the increasing sooting level of fuels, the moderately-sooting n-heptane pool fires are affected by their soot formation with a larger β value. Subsequently, the hot soot particles will progressively play a more important role in the feedback mechanism, as shown from correlated results of heavily-sooting jet-A fires with β =0.27. However, all the current correlated results are smaller than that obtained by De Ris et al, because only the radiation-dominated pool fires were involved in their study. In spite of that, the fact that the influence of flame radiation is magnified with the increasing sooting level for different fuels can be observed.

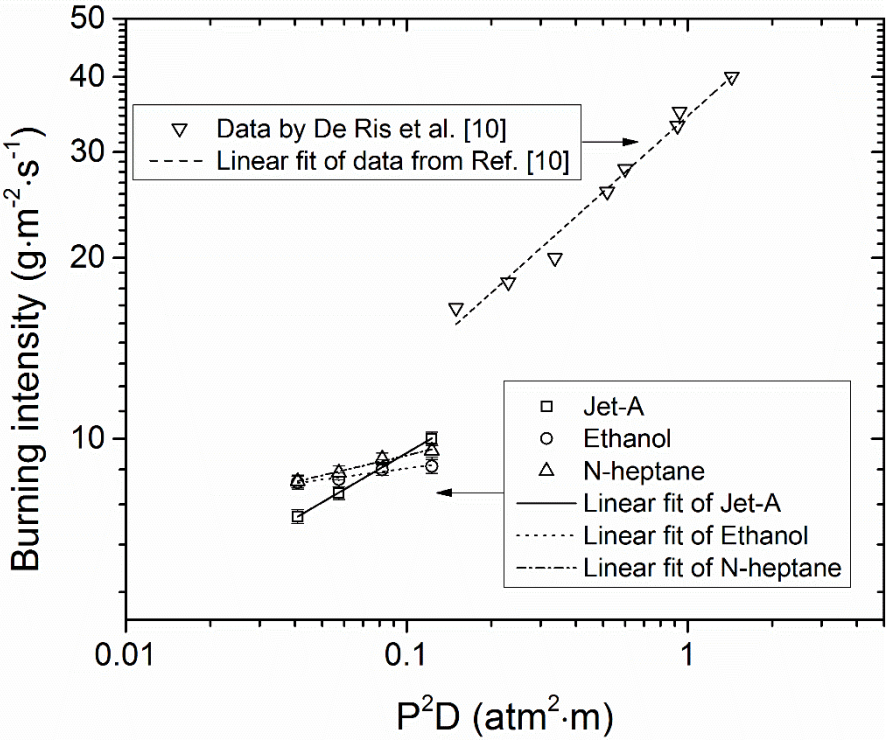

Fig. 4. Burning intensity correlated with radiation modeling

The amount of soot formation in fires is generally characterized as the soot volume fraction f_v, which relates to the power function of ambient pressure, expressed as $f_v \sim P^{\gamma}$. Previous experimental [1-6] and simulative studies [21] jointly predict that the γ values lie in 0.9~2 for turbulent jet flames and fires. Therefore, the soot formation under low pressure will sharply decrease compared with that under normal pressure. The contribution of radiation feedback from soot, however, cannot be neglected under low pressure as the experimental results present, especially for heavily-sooting fuels with a larger slope. Distinguishing the differences of various sooting level fuels will improve the accuracy of application of classical scaling law when performing the similar experiment under different pressures.

3.2 Axial temperature profile

Generally, the axial temperature rise can be scaled by z/z^*, where $z^* = [Q/(\rho_\infty c_p T_\infty \sqrt{g})]^{2/5}$ (Q is fire load which can be calculated from the burning intensity) is introduced as a characteristic length in fire scaling. This scaled relationship can be simplified as $z/Q^{2/5}$ under normal pressure, whereas the ambient air density term ρ_∞ must be involved in correlating with the axial temperature rise under low pressure conditions. As suggested by Zhou et al. [1], the expression $\Delta T \sim z(P/Q)^{2/5}$ can be applied to interpret the axial temperature profiles under different pressures, i.e.

$$\Delta T \sim [z(P/Q)^{2/5}]^{\eta} \tag{4}$$

Three explicit regions of the fire plume are delineated by McCaffrey [22] as flame region ($z/Q^{2/5} < 0.08$), intermittent region ($0.08 < z/Q^{2/5} < 0.2$) and plume region ($z/Q^{2/5} > 0.2$), with η equals to 0, -1, -5/3, respectively in these regions. Given the pressure of 64.3 kPa in Lhasa, the three regions can be further modified as flame region ($zP^{2/5}/Q^{2/5} < 0.42$), intermittent region ($0.42 < zP^{2/5}/Q^{2/5} < 1.06$) and plume region ($zP^{2/5}/Q^{2/5} > 1.06$). Fig. 5 shows the temperature

data measured by different fuels and pool dimensions correlate with $z(P/Q)^{2/5}$, and the data of three tested fuels concentrate and overlap with each other, indicating that the temperature measurements are reasonably reliable.

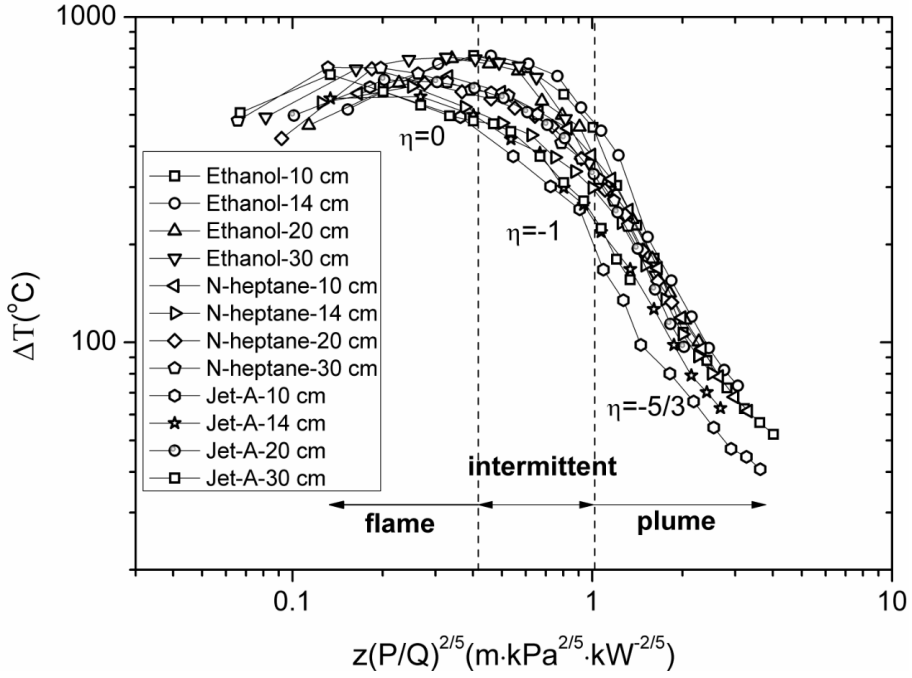

Fig. 5. Averaged axial temperature rise scaled by $z(P/Q)^{2/5}$

A simplified criteria of $T \geq 500\ ^{o}C$ was proposed by Heskestad [23] to identify the flame region and the similar criteria is employed in current study. Fig. 6 plots the averaged flame temperature for different pool dimensions. It clearly shows that the ethanol pool fires possess the highest flame temperature for all pool dimensions, and the temperatures of n-heptane are slightly higher than that of jet-A. This result is in accord with the experimental results under normal pressure. Conventional explanation for this is that as the presence of soot particles in the flame provides the mechanism for radiative heat loss, the "sootier" the flame, the lower its average temperature [24,25]. Consequently, the temperature of the non-luminous alcohol flame is much higher than that of the hydrocarbon flames which lose a considerable proportion of heat by radiation from the soot particles within the flame. This explanation leads to an inference that a larger radiative heat flux is expected for jet-A pool fires.

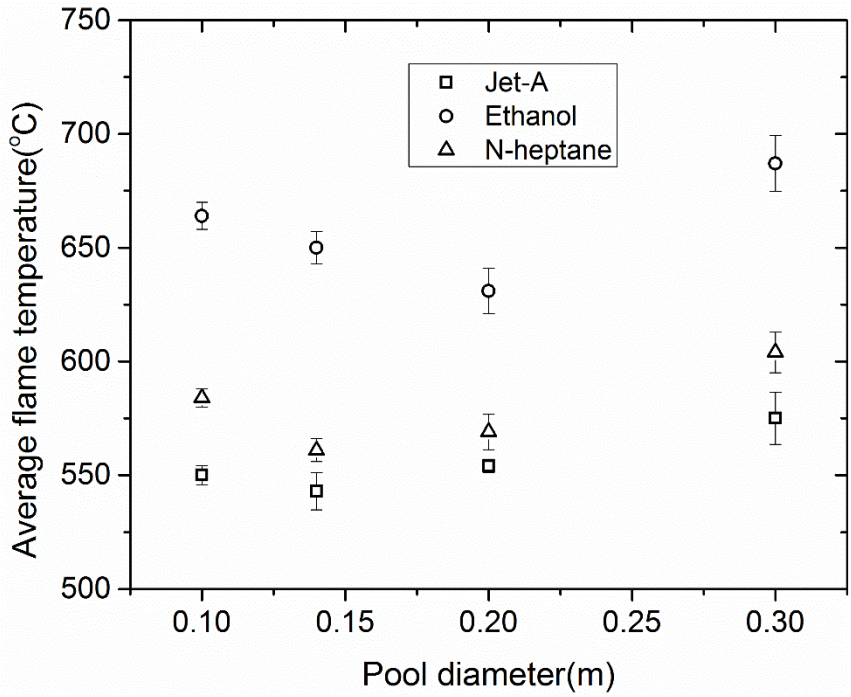

Fig. 6. Averaged flame temperature versus pool dimension

3.3 Radiative heat flux

The radiative heat flux of a flame is usually associated with the flame temperature T_f, the soot absorption coefficient κ and mean beam length L_m [1,25,26], which can be expressed as

$$\dot{q}_r'' = \phi\sigma T_f^4 \left[1 - \exp\left(-\kappa L_m\right)\right] \tag{5}$$

where σ is Stefan-Boltzmann constant, ϕ is the configuration factor from fire to the surface of the radiometer, which is assumed to be unity for all the experimental configurations due to the fixed radiometer position. As the soot production decreases with ambient pressure as a power law relationship (see Section 3.1), κL_m can be reasonably assumed as a small value [1] under low pressure condition. Thus, the Eq. (5) can be approximated as

$$\dot{q}_r'' \approx \phi\sigma\kappa L_m T_f^4 \tag{6}$$

When the soot particle diameter is less than the wave length of radiation, the soot absorption coefficient is related to the soot volume fraction f_v and flame temperature by [2,27]

$$\kappa = 3.72\frac{C_0}{C_2} f_v T_f \tag{7}$$

where C_0 is a constant in the range of 2~6, C_2 is the second Plank constant.

To further evaluate L_m, the time averaged flame shape is assumed to be cylindrical with the diameter equivalent to the burner diameter D and a flame height z_f. In this case, the mean beam length [28] is given as

$$L_m = 0.9\left(\frac{z_f / D}{z_f / D + 1/2}\right)D \tag{8}$$

Though no video records in current study can be processed for the mean flame height, a unified analysis on the flame heights of n-heptane pool fires at different altitudes [1] has demonstrated that the dimensionless flame height z_f/D at high altitude also follows the conventional equation which covers the entire diffusion regime of Q^* ($0.12 < Q^* < 1.2\times10^4$)

$$z_f / D + 1.02 = 3.7\left(Q^*\right)^{2/5} \tag{9}$$

where Q^* is the dimensionless heat release rate [29], expressed as

$$Q^* = \frac{Q}{\rho_\infty c_p T_\infty \sqrt{g} D^{5/2}} \tag{10}$$

Substituting Eqs. (9) and (10) into Eq. (8), the mean beam length can be quantitatively estimated.

Furthermore, combining Eqs. (6)~(8), the radiative heat flux can be estimated as

$$\dot{q}_r'' = C f_v L_m T_f^5 \tag{11}$$

with constant $C = 3.72\phi\sigma C_0 / C_2$. Thus, it has $\dot{q}_r'' \propto L_m T_f^5$ for a fixed fuel. Fig. 7 presents the averaged radiative heat flux in quasi-steady stages versus $L_m T_f^5$, which shows good correlated results for the three fuels and the difference in the slopes definitely demonstrates the inference mentioned above. In fact, the slopes in Fig. 7 represents the dissimilarity of soot volume fraction among fuels with different sooting-levels. Although the soot volume fraction decreases with ambient pressure in the power law relationship, larger slope for higher sooting level fuel manifests that the soot volume fraction under low pressure is still influenced by the characteristics of fuels to a large extent.

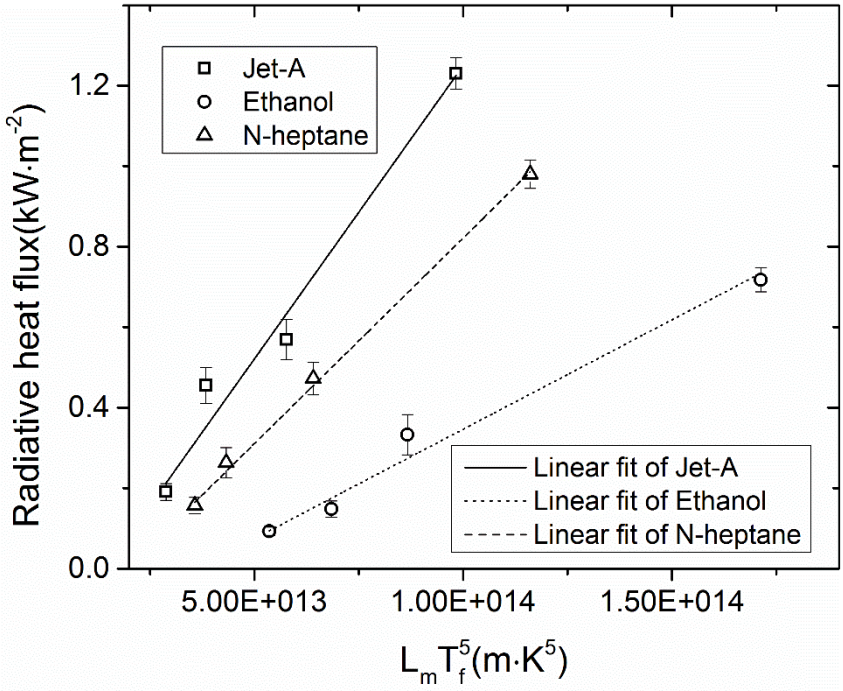

Fig. 7. Linear relationship between radiative heat flux and mass loss for different fuels

4. Conclusions

In this study, three typical liquid fuels with different sooting levels were employed to conduct a series of pool fires in a high altitude city (Lhasa). Conventional scaling laws and theory of fire plume were used to analyze the experimental data. The major conclusions are given as follows:

1. The dimensionless burning intensity $\dot{m}''\mu / D$ can be correlated against the Grashof number at different powers for the three fuels, and the exponent increases with the sooting level of fuels. Non-luminous ethanol flames are more inclined to approach to the theoretical value 1/3 for convention-dominated fires. The radiation modeling also validates this increasing influence caused by higher soot formation.

2. The axial temperature rises scaled by z / z^* are simplified as $\Delta T \sim [z(P/Q)^{2/5}]^{\eta}$, and the demarcation for flame region, intermittent region and plume region are 0.42 and 1.06, respectively, which can well partition the three typical regions of fire plumes in current study. The averaged flame temperature are higher for declined sooting level of fuels, especially for non-luminous ethanol fires. The measured radiative heat fluxes are proportional to the production of $L_m T_f^5$ for different fuels, and the slopes, or the soot volume fraction, increases with the sooting level.

Acknowledgements

This research was supported by the Major Projects of Civil Aviation of China (No. MHRD20130103) and the grant from the Research Grant Council of the Hong Kong Special Administrative Region, China (contract grant number CityU 11301015). The authors deeply appreciate that.

Nomenclature

c_p -specific heat of air, [J kg^{-1} K^{-1}]
C -constant, [-]
D -diameter of the pool, [m]
Fr -Froude number (u^2/gD), [-]
f_v -soot volume fraction, [-]
g -gravitational acceleration, [m s^{-2}]
Gr -Grashof number, [-]
L_m -mean beam length, [m]
$\dot{m}$ -mass loss rate, [g s^{-1}]
$\dot{m}''$ -burning intensity, or mass loss per unit area, [g m^{-2} s^{-1}]
n -exponential factor, [-]
P -pressure, [kPa]
$\dot{q}_r''$ -radiative heat flux, [kW m^{-2}]
Q -heat released, [kW]
Q^* -dimensionless heat release rate, [-]
T_∞ -ambient temperature, [K]
T_f -flame temperature, [K]
z -height above the pool surface, [m]
z^* -dimensionless characteristic length, [-]

z_f -flame height, [m]
ΔH_c -heat of combustion, [kJ kg^{-1}]
α -exponential factor, [-]
β -exponential factor, [-]
γ -exponential factor, [-]
η -exponential factor, [-]
κ -soot absorption coefficient, [m^{-1}]
μ - viscosity, [g s^{-1} m^{-1}]
ρ_∞ -ambient air density, [kg m^{-3}]
σ -Stefan-Boltzmann constant, [W m^{-2} K^{-4}]
ϕ -configuration factor, [-]
χ -radiation fraction, [-]

References

[1] Zhou Z.H., *et al.*, Experimental analysis of low air pressure influences on fire plumes, *International Journal of Heat and Mass Transfer, 70* (2014), pp. 578-585
[2] Li Z.H., *et al.*, Combustion characteristics of n-heptane and wood crib fires at different altitudes, *Proceedings of the Combustion Institute, 32* (2009) 2, pp. 2481-2488
[3] Hu X.K., *et al.*, Combustion characteristics of n-heptane at high altitude, *Proceedings of the Combustion Institute, 33* (2011) 2, pp. 2607-2615
[4] Fang J., *et al.*, Influence of low air pressure on combustion characteristics and flame pulsation frequency of pool fires, *Fuel, 90* (2008), 8, pp. 2760-2766
[5] Tu R., *et al.*, Effects of low air pressure on radiation-controlled rectangular ethanol and n-heptane pool fires, *Proceedings of the Combustion Institute, 34* (2013), 2, pp. 2591-2598
[6] Niu Y., *et al.*, Experimental study of burning rates of cardboard box fires near sea level and at high altitude, *Proceedings of the Combustion Institute, 34* (2013), 2, pp. 2565-2573.
[7] Yao W., *et al.*, Experimental study of large-scale fire behavior under low pressure at high altitude, *Journal of Fire Sciences*, (2013), DOI: 0734904113481326
[8] Wiser D., *et al*., The influence of high altitude on fire detector test fires, *Fire Safety Journal, 29* (1997), 2, pp. 195-204
[9] De Ris J., *et al.*, Pressure modeling of fires, *Proceedings of the Combustion Institute, 14* (1973), 1, pp. 1033–1044
[10] De Ris J., *et al.*, Radiation fire modeling, *Proceedings of the Combustion Institute, 28* (2000), 2, pp. 2751–2759
[11] Alpert R.L., Pressure modeling of transient crib fires, *Combustion Sciences and Technology, 15* (1977), pp. 11-20
[12] Alpert R.L., Pressure modeling of fires controlled by radiation, *Proceedings of the Combustion Institute, 16* (1977), 1, pp. 1489-1500
[13] Zhou Z.H., *et al*., Experimental study of the burning behavior of n-heptane pool fires at high altitude, *Fire and Materials*, (2014), DOI: 10.1002/fam.2270
[14] Luo M.C., *et al.*, Application of field model and two-zone model to flashover fires in a full-scale multi-room single level building, *Fire Safety Journal, 29* (1997), 1, pp. 1-25

[15] Kang Q.S., *et al*., Experimental study on burning rate of small scale heptane pool fires, *Chinese Science Bulletin*, 10 (2010), 55, pp. 973-979.
[16] Liu J.H., *et al*., The burning behaviors of pool fire flames under low pressure, *Fire and Materials*, (2016), 40, pp. 318-334.
[17] Corlett R.C., *et al.*, Pressure scaling of fire dynamics, *Progress in Scale Modeling*, Springer Netherlands, (2008), pp. 85-97
[18] Quintiere J.G., Scaling application in fire research, *Fire Safety Journal*, *15* (1989), pp. 3-29
[19] Kanury A.M., Modeling of pool fires with a variety of polymers, *Proceedings of the Combustion Institute*, *15* (1975), 1, pp. 193-202
[20] Lockwood R.W., *et al.*, Radiative and convective feedback heat flux in small turbulent pool fires with variable pressure and ambient oxygen, In *Proceedings Of the 1987 ASME-JSME Thermal Engineering Joint Conf*., American Society of Mechanical Engineers, New York, USA, 1987
[21] Beji T., *et al.*, A novel soot model for fires: validation in a laminar non-premixed flame. *Combustion and Flame*, *158* (2011), 2, pp. 281-290
[22] McCaffrey B.J., Purely buoyant diffusion flames: some experimental results, National Bureau of Standards, (1979)
[23] Heskestad G., Virtual origin of fire plume, *Fire Safety Journal*, *5* (1983), 2, pp. 109-114
[24] Matthews L., *et al*., Radiative flux measurements in a sooty pool fire, *Experimental Heat Transfer*, *2* (1989), 3, pp. 189-199
[25] Drysdale D., *An introduction to fire dynamics* (*2nd edition*), John Wiley & Sons Ltd., New York, USA, 1999
[26] De Ris J., Fire radiation- a review, *Symposium (International) on Combustion*, 17 (1979), 1, pp. 1003-1016
[27] Shinotake A., An experimental study of radiative properties of pool fires of an intermediate scale, *Combustion Science and Technology*, 43 (1985), 1-2, pp. 85-97
[28] Zarzecki M., The effect of pressure and oxygen concentration on the combustion of PMMA, *Combustion and Flame*, 160 (2013), 8, pp. 1519-1930
[29] Zukoski E.E., Visible structure of buoyant diffusion flames, *Proceedings of the Combustion Institute*, 20 (1985), 1, pp. 360-366